ELSEVIER

Journal of Archaeological Science 32 (2005) 1061–1075

Journal of Archaeological SCIENCE

http://www.elsevier.com/locate/jas

$^{87}Sr/^{86}Sr$ sourcing of ponderosa pine used in Anasazi great house construction at Chaco Canyon, New Mexico

Amanda C. Reynolds[a,*], Julio L. Betancourt[b], Jay Quade[a], P. Jonathan Patchett[a], Jeffrey S. Dean[c], John Stein[d]

[a]*Department of Geosciences, University of Arizona, Tucson, AZ 85721, USA*
[b]*U.S. Geological Survey, 1675 W. Anklam Road, Tucson, AZ 85745, USA*
[c]*Laboratory of Tree-Ring Research, University of Arizona, Tucson, AZ 85721, USA*
[d]*Navajo Nation, Chaco Protection Sites Program, 2105 East Aztec Avenue, Gallup, NM 87301, USA*

Received 4 October 2004; received in revised form 27 January 2005

Abstract

Previous analysis of $^{87}Sr/^{86}Sr$ ratios shows that 10th through 12th century Chaco Canyon was provisioned with plant materials that came from more than 75 km away. This includes (1) corn (*Zea mays*) grown on the eastern flanks of the Chuska Mountains and floodplain of the San Juan River to the west and north, and (2) spruce (*Picea* sp.) and fir (*Abies* sp.) beams from the crest of the Chuska and San Mateo Mountains to the west and south. Here, we extend $^{87}Sr/^{86}Sr$ analysis to ponderosa pine (*Pinus ponderosa*) prevalent in the architectural timber at three of the Chacoan great houses (Pueblo Bonito, Chetro Ketl, Pueblo del Arroyo). Like the architectural spruce and fir, much of the ponderosa matches the $^{87}Sr/^{86}Sr$ ratios of living trees in the Chuska Mountains. Many of the architectural ponderosa, however, have similar ratios to living trees in the La Plata and San Juan Mountains to the north and Lobo Mesa/Hosta Butte to the south. There are no systematic patterns in spruce/fir or ponderosa provenance by great house or time, suggesting the use of stockpiles from a few preferred sources. The multiple and distant sources for food and timber, now based on hundreds of isotopic values from modern and archeological samples, confirm conventional wisdom about the geographic scope of the larger Chacoan system. The complexity of this procurement warns against simple generalizations based on just one species, a single class of botanical artifact, or a few isotopic values.

Keywords: Provenance; Botanical; Strontium isotopes; Architectural timber; Chaco Canyon; San Juan Basin; Southwestern U.S.A.

1. Introduction

In the southwestern U.S.A., strontium (Sr) isotopic analyses of archeological bone and plant tissue are being used increasingly to decipher prehistoric migration patterns, residential shifts in population [29], and long-distance procurement of timber [17] and foodstuffs [4]. Strontium exists in predictable and measurable quantities in rocks and sediment, as well as in plant matter, bones, and teeth recoverable from archeological sites. The ratio of ^{87}Sr to ^{86}Sr isotopes is maintained from soil water, through plants, and up the trophic chain, making it ideal for provenance studies [8].

Architectural timber common in southwestern ruins is particularly well suited for $^{87}Sr/^{86}Sr$ analysis. In most cases, the abundant and well-preserved logs have been identified to species, their architectural function

* Corresponding author. Tel.: +1 520 621 4532; fax: +1 520 670 6806.
E-mail address: reynolds@geo.arizona.edu (A.C. Reynolds).

0305-4403/$ - see front matter © 2005 Elsevier Ltd. All rights reserved.
doi:10.1016/j.jas.2005.01.016

and placement have been established, and their cutting dates have been determined to the exact year, depending on the condition of the timber. This dated and well-provenienced wood has been archived and is readily accessible for geochemical studies. Probably the richest such archive is associated with more than a century of excavations at Chaco Canyon, New Mexico [14,23,35,36]. Construction of the great houses at Chaco Canyon required over 200,000 highland conifers, including spruce (*Picea* spp.), fir (*Abies* spp.), Douglas-fir (*Pseudotsuga menziesii*), and ponderosa pine (*Pinus ponderosa*) [14].

Paradoxically, Chaco Canyon is set in desertscrub-grassland in the middle of the San Juan Basin and removed at least 75 km from the nearest potential timber sources (Figs. 1 and 2). The packrat midden record indicates that highland conifers were either absent locally, as in the case of spruce and fir, or too rare, as in the case of Douglas-fir and ponderosa pine, to have provisioned the Anasazi (prehistoric Puebloans) builders of the Chacoan great houses [6]. Most of this wood had to be felled, processed, harvested and hauled from one or more distant highland areas [5]. The distances and directions of sources for timber procurement are one measure of economic, political and social relationships across the San Juan Basin. Location of the source stands can be narrowed somewhat by species (i.e., spruce and fir grow only on some mountaintops), but more specific locations require application of geochemical tracers.

Diverse rock types with diverse chemical signatures characterize the San Juan Basin and surrounding

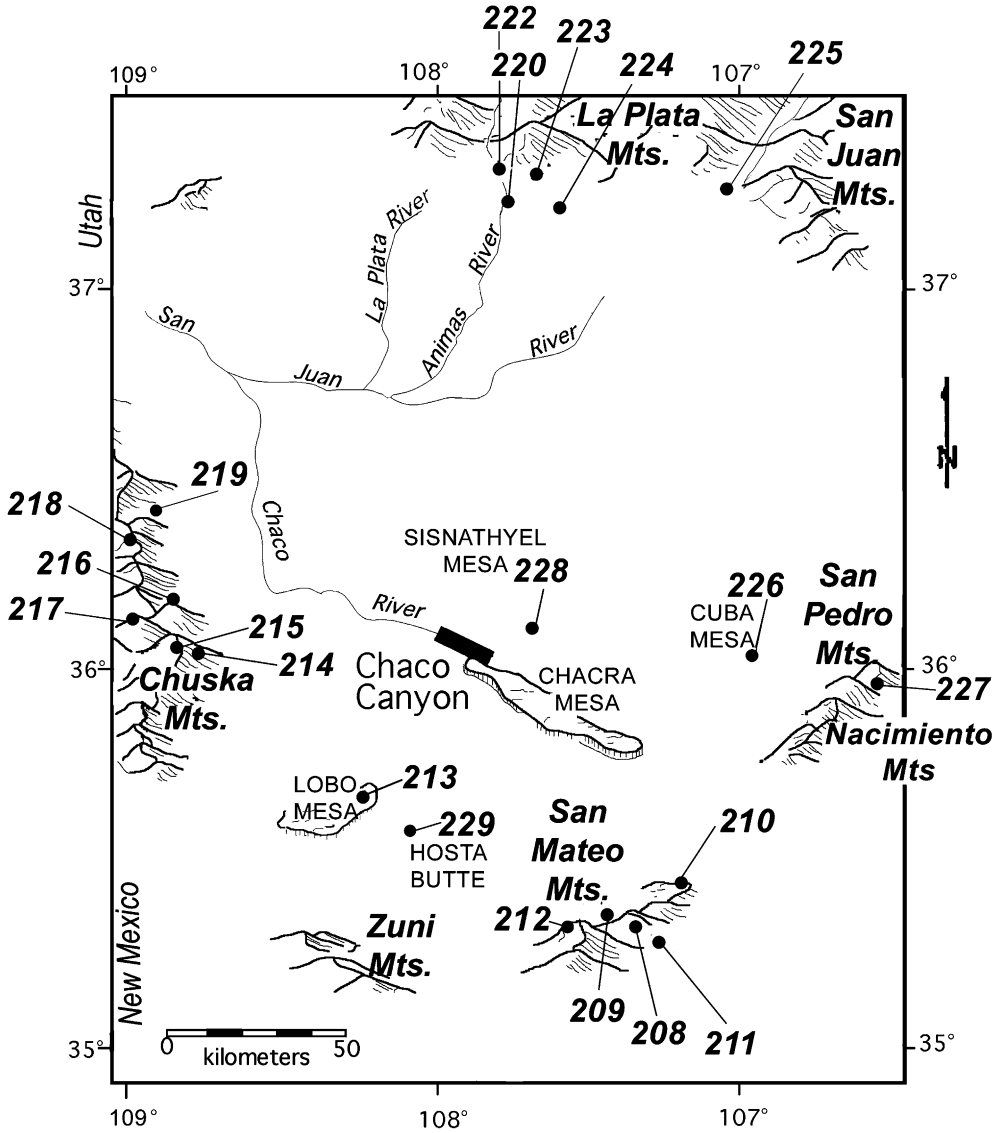

Fig. 1. Map of San Juan Basin showing potential source stands of modern ponderosa pine that were sampled for $^{87}Sr/^{86}Sr$ analysis. 208–229 represent sampling site numbers (see Table 1). Adapted from Kantner [24].

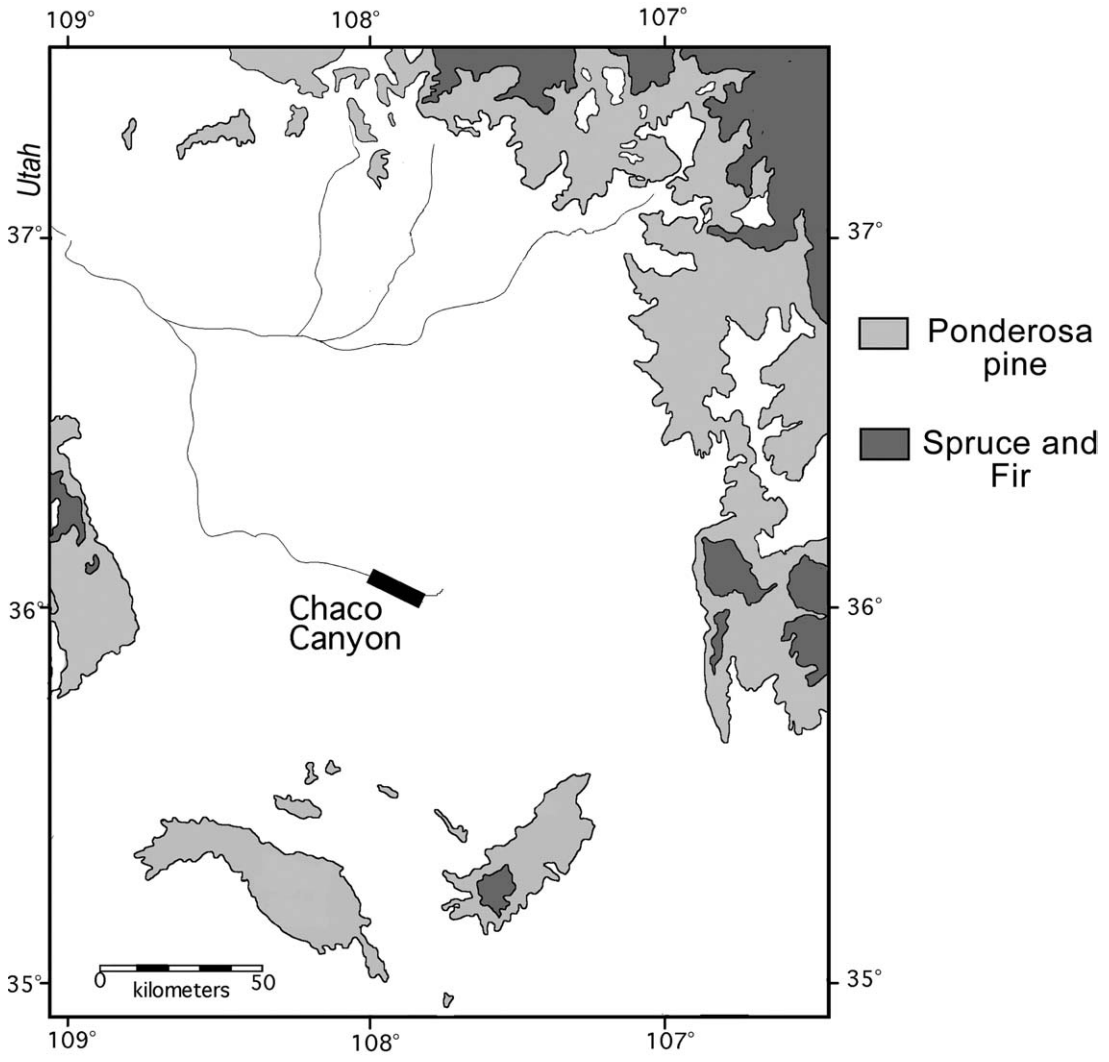

Fig. 2. General map of spruce–fir and ponderosa pine forest distribution in the San Juan Basin. Modified from English et al. [17].

highlands, particularly the mountaintops (Fig. 3). The Chuska Mountains west of Chaco Canyon are a north–south trending range capped with Tertiary sandstone, locally overlain by Tertiary basalt. The San Mateo Mountains (also referred to as Mt. Taylor) to the south represent a succession of lava and ash flows erupted 2–4 million years ago. The San Pedro/Nacimiento Mountains to the east are composed of highly faulted blocks of Precambrian crystalline rock, of diverse composition, overlain in places by Paleozoic sedimentary rocks. The La Plata Mountains to the north are composed of a Cretaceous granitic batholith capped by Tertiary sedimentary basin deposits. Sandstones and shales of various ages and composition flank each of the four ranges.

A preliminary study by Hatch [20] used inductively coupled plasma-atomic emission spectrometry to characterize 77 modern ponderosa pine from Chimney Rock and 52 architectural samples from Chimney Rock, Aztec, and Salmon Ruins. Hatch [20] found higher elemental concentrations in the prehistoric samples suggesting elemental contamination with burial. Hatch [20] recognized that differences in elemental concentrations between different wood species and different wood compositions (sapwood versus heartwood and living versus dead wood) needed to be constrained in her results before secondary contamination could be quantified in the architectural wood samples. Also, the authors did not address the effects of pretreatment and drying methods on wood elemental concentrations.

Durand et al. [16] conducted a study of 28 major and trace elements in wood of 62 ponderosa pine and Douglas-fir trees growing on three bedrock types (basalt, sandstone and shale) in the San Juan Basin. The authors recognized heartwood elemental concentrations to be more reliable than sapwood for trace element studies of wood. Durand et al. [16] suggested that barium concentrations in architectural wood tend

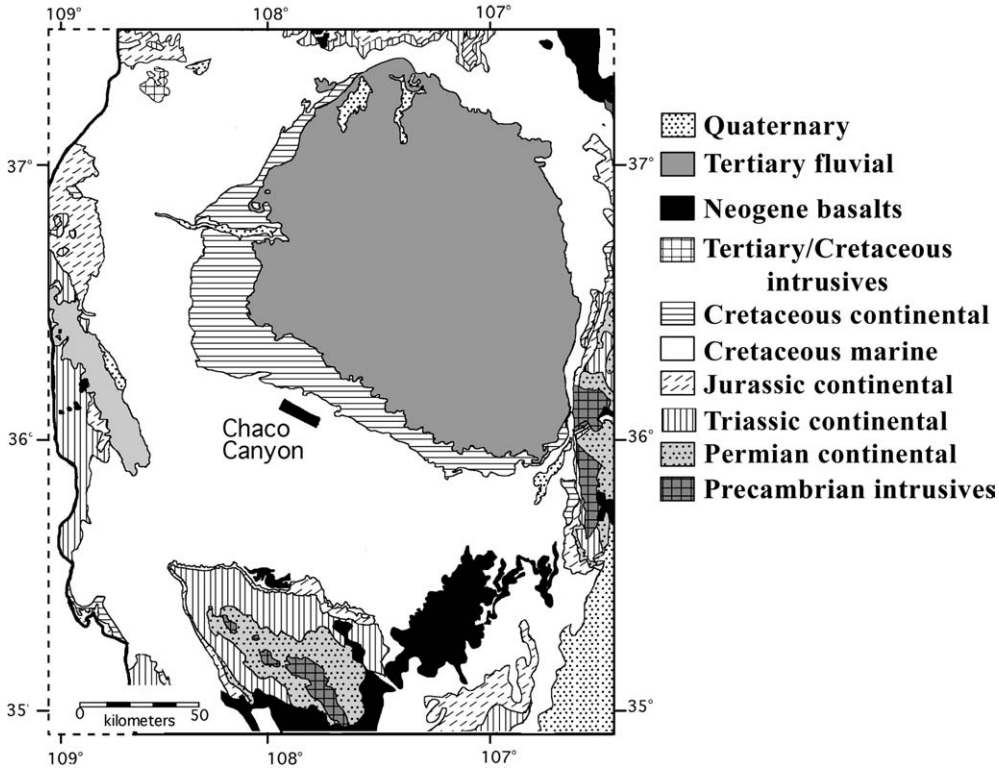

Fig. 3. Generalized geologic map of the San Juan Basin. Adapted from Craigg [12].

to vary with relative mobility of barium for different lithologies, with high mobility in sandstones and low in basalts. Low barium concentrations in 13 ponderosa pine beams from Chacoan great houses suggested a source in either San Mateo or the Chuska Mountains, both capped at least in part by Neogene basalts (Fig. 3). The authors admitted that more research needed to be done to conclusively source the architectural timbers using elemental concentrations due to the lateral, differential movement of most elements in sapwood [3,9,15,26,31]. The study shows, however, that less mobile elements such as barium may be useful in sourcing studies.

English et al. [17] narrowed the search for Chacoan wood sources by reasoning that trees assimilate Sr from local soils and atmospheric dust and incorporate it into wood without fractionating the isotopes ^{87}Sr and ^{86}Sr. The $^{87}Sr/^{86}Sr$ ratio in the wood should be independent of the vital effects controlling fluctuations in elemental concentrations and solely reflect the ratio in local soil water, which is some combination of local weathering products and atmospheric dust [18]. English et al. [17] also narrowed the search by focusing on spruce and fir, which are restricted today to only a few widely separated and geologically distinct mountaintops.

English et al. [17] analyzed $^{87}Sr/^{86}Sr$ ratios in wood of 73 living spruce and fir trees from three mountain ranges (Chuska, San Mateo, and San Pedro/Nacimiento Mountains) within 100 km of Chaco Canyon. Despite the presence of a "Great North Road" [34], they excluded sampling the La Plata and San Juan Mountains to the north because those spruce–fir forests were most distant (>150 km) and least accessible, requiring transport of large beams across deep canyons and flowing rivers. Trees from the Chuska, San Mateo and San Pedro/Nacimiento Mountains each exhibited distinguishable $^{87}Sr/^{86}Sr$ ratios.

English et al. [17] also measured 52 architectural specimens of spruce and fir from several great houses in Chaco Canyon (Pueblo Bonito, Chetro Ketl, Pueblo del Arroyo, Wijiji, Hungo Pavi and Una Vida). Two-thirds of the architectural specimens could be traced to the Chuska Mountains and one-third to the San Mateo Mountains. The two fingerprinted sources were both logged as early as A.D. 974, suggesting that selection of timber sources was driven more by socioeconomic ties with communities to the west and south than by timber depletion with distance and time. Conversely, the absence of logs from the San Pedro/Nacimiento Mountains is consistent with the lack of roads and paucity of outlying Chacoan communities to the east. The importance of the Chuska Mountains for resource procurement was recently confirmed by $^{87}Sr/^{86}Sr$ analysis of prehistoric corn from Chaco Canyon [4]. This study, however, points to the San Juan floodplain as an additional source of corn.

Here we extend the Chaco Sr isotope work to ponderosa pine. Ponderosa pine is more widely distributed than spruce and fir and stands occur within 100 km of Chaco Canyon in all directions. Therefore, we expanded the original geographic scope of English et al. [17] to encompass sampling of live trees in the La Plata and San Juan Mountains, and previously unsampled mesas (e.g., Hosta Butte and Lobo, Cuba and Sisnathyel Mesas; Fig. 1) and mountain flanks throughout the San Juan Basin. Ponderosa pines grow at lower elevations and in closer proximity to Chaco Canyon than spruce and fir, so ponderosa might have been used earlier and from a wider variety of geologic settings and elevations. Moreover, ponderosa pine represents more than half of the estimated 200,000 timbers employed in great house construction [14], and may further constrain exploitation of different timber sources. For example, the abundance of trees in size classes desirable for Chacoan architecture was restricted by substrate, elevation, slope aspect and grade, which mediate interspecific competition and rates of ecological disturbance, tree mortality, and recruitment. Smaller secondary beams may have been acquired from fast-growing stands in the moister highlands, while larger primary beams could have come from more open and fire-prone parklands on mesas and foothills characterized by a few mature trees and a scarcity of saplings.

2. Technical background

2.1. Sr isotopes

Sr is an alkaline earth element that has the same charge and a similar atomic radius to calcium and thus commonly substitutes for Ca in chemical reactions. Sr has four stable, naturally occurring isotopes with different abundance: ^{84}Sr (0.6%), ^{86}Sr (9.9%), ^{87}Sr (7.0%), and ^{88}Sr (82.6%). $^{87}Sr/^{86}Sr$ ratios are commonly reported in geochemical investigations. The $^{87}Sr/^{86}Sr$ ratio of minerals is mostly a function of the initial $^{87}Rb/^{86}Sr$ ratio and the age of the rock. ^{87}Sr is radiogenic, derived from the radioactive decay of rubidium-87 ($t_{1/2}$ = 48.8 Ga). Rocks that are older or have higher initial concentrations of ^{87}Rb will yield higher $^{87}Sr/^{86}Sr$ ratios. The utility of $^{87}Sr/^{86}Sr$ ratios as a tracer comes from the fact that, in a closed system, the $^{87}Sr/^{86}Sr$ ratio of secondary clay minerals will be the same as that in the original, unweathered mineral. The $^{87}Sr/^{86}Sr$ ratios of local rocks, dust and precipitation are integrated by hydrologic processes and can be estimated by measuring $^{87}Sr/^{86}Sr$ ratios in stream waters (e.g. [10]), which should approximate the $^{87}Sr/^{86}Sr$ ratio available to plants.

Within the 21,600-km^2 San Juan Basin, bedrock units display a wide range of $^{87}Sr/^{86}Sr$ isotopic ratios due to their age, composition, and formation history. Precambrian crystalline rocks and Neogene basalts lie on two ends of a spectrum. Small and sparse outcrops of Precambrian granite with characteristically higher $^{87}Sr/^{86}Sr$ ratios (0.8043–0.8644) [33] are exposed to the northwest, east, and southwest and dominate the Sr inventory in those regions of the basin (see Fig. 3). Neogene basalts, which yield moderately low $^{87}Sr/^{86}Sr$ ratios (0.7023–0.7142) [13], are the dominant bedrock in the San Mateo Mountains to the southeast and occur sporadically along the crest of the Chuska Mountains. Most of the San Juan Basin is underlain by marine and terrestrial sedimentary units whose $^{87}Sr/^{86}Sr$ ratios fall between the two extremes.

Chaco Canyon is situated at the boundary between Cretaceous marine deposits (whole rock value of 0.7075 in Ref. [27]) and Cretaceous and Tertiary fluvial deposits (values for ground water 0.7083–0.7093). Fine sediment from these extensive fluvial deposits may contribute heavily to Sr in the regional atmospheric dust load. At Chaco Canyon itself, uniformity in plant and animal $^{87}Sr/^{86}Sr$ ratios confirms the dominance of atmospheric inputs to the surficial Ca and Sr cycles in the region. The aeolian component of sediment deposited in Werito's Rincon, a deep alcove along the south wall of Chaco Canyon, yielded $^{87}Sr/^{86}Sr$ values ranging from 0.7095 to 0.7096 [4]. Bones from modern rodents in Chaco Canyon yielded a mean $^{87}Sr/^{86}Sr$ of 0.7095 ± 0.0002 (Reynolds, Betancourt and Akins, unpublished data). Soil water values for Chaco Canyon, estimated from leaching studies, range from 0.70896–0.70961 [4].

2.2. Strontium isotopes and plants

Rooting depths and depth of available soil water will greatly influence the $^{87}Sr/^{86}Sr$ of plants. $^{87}Sr/^{86}Sr$ ratios in flora directly reflect the $^{87}Sr/^{86}Sr$ of the soil water, which, in turn, is determined by the relative contributions of local bedrock weathering and regional atmospheric dust [1,7,18,19,30]. Sr contributions to the soil water from bedrock weathering is greater in rocks where there are more reactive minerals (e.g. salt) or where mineral surface area is large due to smaller grain size. Conversely, soils that are older [11], in regions of higher precipitation [32], and shallower [1,2] are more likely to reflect the $^{87}Sr/^{86}Sr$ of atmospheric inputs. Additions of isotopically-distinct water to a forest site in Chile revealed vertical variations in a soil water column, with shallow soil layers dominated by atmospheric contributions and mineral weathering governing much deeper sections of soil [25]. The Chilean study also found that the atmospherically dominated soil layers have the potential for overturning and changing $^{87}Sr/^{86}Sr$ ratios on decadal timescales.

In the southwestern U.S., however, where atmospheric input dominates the Sr cycle, Sr isotopic values

in plants should vary less in time and space. In the Sangre de Cristo Mountains near Taos, New Mexico, $^{87}Sr/^{86}Sr$ ratios in wood and leaf cellulose from spruce, fir and aspen were used to study chemical weathering, atmospheric deposition and solute acquisition [18,19]. Some major findings include homogeneity of $^{87}Sr/^{86}Sr$ ratios from biomass measurements across individual trees, different species and soil water at the same site; rapid biological cycling relative to Sr input into the ecosystem across the stand; and an overriding influence of atmospheric dust (75%) over local weathering (25%) as the source of bioavailable Sr in soil waters and tree biomass. In addition, pedogenic carbonate dominates aeolian Ca and Sr cycles producing more uniform aeolian dust compositions. $^{87}Sr/^{86}Sr$ ratios from soil carbonate formed on basalts of different ages demonstrate that the composition of aeolian dust must have remained stable over the last several million years [28]. In the San Pedro/Nacimiento Mountains near Cuba, New Mexico, conifer $^{87}Sr/^{86}Sr$ ratios vary little despite growing on three different substrates (granite, limestone, and sandstone) [17]. This probably reflects the overriding influence of the widely exposed granite with higher $^{87}Sr/^{86}Sr$ ratios on regional atmospheric dust sources of Sr, which trees recycle over decades to centuries.

Naiman et al. [28] suggest that, in the southwestern U.S., $^{87}Sr/^{86}Sr$ ratios of atmospheric dust vary at most on a scale of 200–300 km, although this was roughly the resolution of their sampling. This scale of mixing would tend to homogenize $^{87}Sr/^{86}Sr$ within mountain ranges, while producing the distinct ratios between lithologically-contrasting mountain ranges, as we observe in this study. We recognize, however, that the range of $^{87}Sr/^{86}Sr$ ratios across any particular mountain range will increase with sampling intensity, as more local substrate variations are encountered. On the other hand, not every site has an equal chance of having been logged by the Anasazi. For example, we made a concerted effort to sample sites that would have been most acceptable to the Anasazi, particularly with regards to ease of logging and transport.

3. Methods

3.1. Sampling of living trees to establish baseline for provenance studies

In the summer of 2002, we sampled more than 200 living trees from 20 localities in the La Plata Mountains, San Juan Mountains, Sisnathyel Mesa, Cuba Mesa, San Pedro/Nacimiento Mountains, San Mateo Mountains, Lobo Mesa, Hosta Butte and Chuska Mountains. All living trees were cored at breast height with a ¼-inch increment borer. No lubricants were used to avoid chemical contamination. Individual trees were chosen from stands growing on a diverse array of bedrock types. Five individual tree cores were taken from each locale to characterize variation within the stand. Sampled trees varied in diameter and age. We generally avoided topographic lows where trees could access shallow ground water. At most sites, we only sampled ponderosa pine. In the La Plata and San Juan Mountains, however, we also sampled spruce, fir and aspen to fill the gap in sampling from English et al. [17].

3.2. Sampling of architectural samples

All of the samples of architectural timber came from the collection stored at the Laboratory of Tree Ring Research at the University of Arizona. Ponderosa pine primary and secondary beams of known age were analyzed from Pueblo Bonito, Chetro Ketl, and Pueblo del Arroyo, mostly from periods of increased construction activity [35,36]. Samples were selected to determine use of general stockpiles, or reliance on specific source areas for particular construction periods, individual great houses, or specific rooms within a great house. Samples were also taken from eight beams original to Chaco Canyon, but whose provenience is complicated by their reuse in National Park Service (NPS) modern stabilization efforts. These eight beams, noted by "nps" in Table 2, are placed under their original great house based on NPS notes. At least some of these beams came from a flood-damaged section of Chetro Ketl [14].

We also analyzed a dead ponderosa that Judd [23, pp. 39–40] described from the West Plaza of Pueblo Bonito: "The JPB-99 of our list is from a much decayed pine that had stood at the south end of the West Court while Pueblo Bonito was inhabited. Initially Douglass (1935, p. 47) gave this fragment a tentative date of A.D. 1017±35, but in a later review Smiley fixed the outermost surviving ring at 983. One may only guess at the number of annual rings lost through disintegration but that lone, midvalley straggler from the Chaco forest obviously witnessed the unfolding of much Pueblo Bonito history." JPB-99s inside ring (A.D. 732±) is far from the pith; therefore, this tree could have easily germinated in the late 7th century, long before the start of construction at Pueblo Bonito. Its outer ring dates at A.D. 981, but that is not a cutting date, and the tree undoubtedly died long thereafter.

Clearly, Judd did not think that this tree was actually planted by the residents of Pueblo Bonito. Rather, he viewed it as a forlorn remnant of a pine forest he presumed blanketed Chaco Canyon and vicinity before being eradicated by Chaco residents in search of construction beams. There are in fact a few dozen living ponderosa pines in three stands in or near Chaco Canyon: (1) on the cliff just above and east of Casa Rinconada; (2) ~30 km north of Pueblo Bonito along

Ojo Alamo Wash and De-na-zin Wash in the Bisti Badlands, and (3) ~25 km southeast of Pueblo Bonito on Chacra Mesa. These stands were surveyed in 1970–1971 by Gwinn Vivian (notes on file at the National Park Service) and were revisited by Julio Betancourt in the early 1980s. Despite these few living trees, we know from the local packrat midden record [6] that ponderosa pine never grew in sufficient numbers (10^4–10^5 trees) to have provisioned Chacoan great houses such as Pueblo Bonito. Here we will use the $^{87}Sr/^{86}Sr$ ratio of the "rooted" tree in the West Plaza of Pueblo Bonito to include or rule out Chaco Canyon as one of the possibilities for its growing environment.

3.3. $^{87}Sr/^{86}Sr$ measurements

Both modern and ancient trees were processed similarly, with the exception that architectural beams were treated ultrasonically in high-purity milli-Q water to remove any diagenetic (secondary) salts. We sampled the innermost (earliest) rings of sections of cores from both modern and prehistoric tree samples. The outermost 1–2 mm of the core's surface was physically removed and discarded to prevent contamination due to handling, storage processes, or diagenesis (in semi-arid environments like Chaco Canyon, evaporation of local soil water could lead to deposition Sr-rich salts inside archeobotanical materials). A total of 60–100 mg of wood was then cut into 1–2 mm^3 pieces and placed in an acid-cleaned Vycor tube. Samples were combusted between 750 and 850 °C for 12–18 h until all organic matter was ashed. Samples were then transported to a clean lab for wet chemical processing. The remaining inorganic ash was dissolved in distilled 6 M HCl, transferred to a Teflon vial, and an ^{84}Sr tracer was added to allow determination of Sr concentration. Samples were dried down on a hotplate, redissolved in 3.5 M HNO_3, and run through Eichrom Sr-specific resin columns to isolate the strontium from the sample. Samples were analyzed for $^{87}Sr/^{86}Sr$ and Sr concentration on a thermal ionization mass spectrometer (TIMS) at the University of Arizona. NBS-987 standards were analyzed repeatedly, yielding an $^{87}Sr/^{86}Sr$ ratio of 0.710268 ± 0.00004 ($n = 24$).

To test for diagenetic effects, Sr concentrations were corrected for differences in water content using bulk density measurements. The dry architectural samples yielded an average bulk density of 0.230 ± 0.08 g/cm^3. Living trees were adjusted for water loss so that they could be compared to architectural wood. The following equation was used:

$$ppm_{corr} = \frac{BD_{live} \times ppm_{meas}}{BD_{average}}$$

where ppm_{corr}, corrected concentration in modern wood; BD_{live}, bulk density of modern tree at the time of sampling for chemical analysis; ppm_{meas}, concentration measured on TIMS using ^{84}Sr tracer; $BD_{average}$, average bulk density for architectural specimens (0.23 g/cm^3).

4. Results

4.1. $^{87}Sr/^{86}Sr$ variations in living trees from potential source areas

Sixty-two living ponderosa, and three subalpine fir (*Abies lasiocarpa*, *Abies concolor*), two aspen (*Populus tremuloides*), and two Engelmann spruce (*Picea engelmannii*) were analyzed to characterize $^{87}Sr/^{86}Sr$ variations across 21 potential source stands (Fig. 1). The firs and spruce were sampled from the La Plata and San Juan Mountains, which were previously excluded from the range of sites sampled by English et al. [17]. $^{87}Sr/^{86}Sr$ values for the living trees ranged from 0.7055 to 0.7192 (Table 1; Fig. 4). The highest $^{87}Sr/^{86}Sr$ ratios (>0.7139) characterize Cuba Mesa (226 in Fig. 1, Table 1) and the San Pedro/Nacimiento Mountains (227). The La Plata Mountains (220, 222, 223 and 224), San Juan Mountains (225), Lobo Mesa (213), and Hosta Butte (229) yielded lower average $^{87}Sr/^{86}Sr$ ratios (0.7094–0.7115, excluding an *Abies* sample from site 222 with $^{87}Sr/^{86}Sr = 0.7086$), followed by the Chuska Mountains (214–219:0.7071–0.7098) and the San Mateo Mountains (208–212:0.7060–0.7086). There was slight overlap in ratios (0.7094–0.7097) between the Chuska and the La Plata Mountains, but only at Chuska sites north of site 216 (Fig. 1). There was no overlap, however, between the ratios from the Chuska Mountains and sites on Lobo Mesa, Hosta Butte, or Sisnathyel Mesa, which have similar values to the La Plata and San Juan Mountains.

4.2. $^{87}Sr/^{86}Sr$ variations in architectural samples

Fifty-three architectural ponderosa and one *Populus* (either cottonwood or aspen) spanning A.D. 919–1101 were analyzed for $^{87}Sr/^{86}Sr$ ratios (Table 2; Fig. 5). Beams from restabilization efforts are categorized according to their noted "original" location (see Table 2). Most of the architectural ponderosa fall within the range of 0.7071–0.7113, except two samples with high values [ck-1300, a secondary beam from Chetro Ketl ($^{87}Sr/^{86}Sr = 0.7170$) and ckk-72, a lintel-sized NPS stabilization beam ($^{87}Sr/^{86}Sr = 0.7157$)]. The only matches for these high values among living trees are the San Pedro/Nacimiento Mountains and Cuba Mesa. Of the 52 architectural ponderosa, 35% overlapped with the range of values (0.7098–0.7115) for living trees in the La Plata Mountains, San Juan Mountains, Hosta Butte and Lobo Mesa. Approximately 35% of architectural

Table 1
Summary of baseline site information, $^{87}Sr/^{86}Sr$ ratios, and Sr concentration from living ponderosa pine (and at one site, spruce and fir) in the San Juan Basin

Site		$^{87}Sr/^{86}Sr$*	2σ	Sr_{wood} (ppm)	BD_{wood}	$Sr^{1}_{corrected}$ (ppm)
San Mateo Mountains						
Site 208 N35°15.795′ W107°37.978′ 2843 m						
P. ponderosa	sm-208a	0.70596	6	6.3	0.35	7.3
P. ponderosa	sm-208d	0.70601	9	1.7	0.69	3.9
Site 209 N35°17.126′ W107°36.186′ 2410 m						
P. ponderosa	sm-209a	0.70774	15	5.5	0.51	9.4
P. ponderosa	sm-209b	0.70779	27	8.4		
P. ponderosa	sm-209c	0.70819	7	12.1	0.48	19.2
P. ponderosa	sm-209d	0.70768	9	11.2		
Site 210 N35°21.787′ W107°32.707′ 2480 m						
P. ponderosa	sm-210b	0.70550	5	6.4		
P. ponderosa	sm-210c	0.70744	9	7.0		
P. ponderosa	sm-210d	0.70745	18	9.0		
P. ponderosa	sm-210e	0.70712	8	8.9	0.75	22.4
Site 211 N35°21.788′ W107°32.707′ 2406 m						
P. ponderosa	sm-211a	0.70686	8	7.0		
P. ponderosa	sm-211b	0.70698	10	4.1		
P. ponderosa	sm-211d	0.70855	24	6.1		
Site 212 N35°16.170′ W107°43.313′ 2519 m						
P. ponderosa	sm-212b	0.70702	4	8.6		
P. ponderosa	sm-212c	0.70713	4	5.5	0.42	7.7
P. ponderosa	sm-212e	0.70680	8	6.7	0.42	9.5
Lobo Mesa						
Site 213 N35°37.928′ W108°13.374′ 2283 m						
P. ponderosa	lm-213f	0.71150	17	2.4	0.82	6.7
Chuska Mountains						
Site 214 N36°05.757′ W108°51.147′ 2534 m						
P. ponderosa	chm-214b	0.70706	2	7.4		
P. ponderosa	chm-214d	0.70713	17	10.8	0.48	17.2
Site 215 N36°04.810′ W108°53.028′ 2531 m						
P. ponderosa	chm-215a	0.70914	2	7.6	0.32	8.2
P. ponderosa	chm-215b	0.70917	12	3.0		
P. ponderosa	chm-215c	0.70892	19	5.0	0.38	6.4
P. ponderosa	chm-215d	0.70913	10	4.6	0.39	6.0
P. ponderosa	chm-215e	0.70940	26	4.7	0.69	10.8
Site 216 N36°04.810′ W108°53.028′ 2698 m						
P. ponderosa	chm-216a	0.70870	24	4.1	0.43	5.9
P. ponderosa	chm-216b	0.70841	11	3.0		
P. ponderosa	chm-216c	0.70856	8	3.0	0.42	4.2
P. ponderosa	chm-216d	0.70926	9	7.5	0.38	9.4
Site 217 N36°10.099′ W108°56.618′ 2740 m						
P. ponderosa	chm-217d	0.70935	10	6.0	0.52	10.4
Site 218 N36°15.590′ W108°56.310′ 2487 m						
P. ponderosa	chm-218a	0.70967	13	2.0		
P. ponderosa	chm-218b	0.70958	21	5.0	0.34	5.7
P. ponderosa	chm-218c	0.70955	38	1.1	0.42	1.6
P. ponderosa	chm-218d	0.70951	12	3.8	0.38	4.9
P. ponderosa	chm-218e	0.70946	11	4.5	0.38	5.6
Site 219 N36°14.599′ W108°54.715′ 2301 m						
P. ponderosa	chm-219a	0.70974	8	18.1		
P. ponderosa	chm-219b	0.70950	12	2.7	0.62	5.6
P. ponderosa	chm-219d	0.70952	9	6.0	0.54	10.7
P. ponderosa	chm-219e	0.70957	16	12.0	0.53	21.3

Table 1 (*continued*)

Site		$^{87}Sr/^{86}Sr^*$	2σ	Sr_{wood} (ppm)	BD_{wood}	$Sr^{1}_{corrected}$ (ppm)
Hosta Butte						
Site 229 N35°35.287′ W108°48.612′ (UTM in zone 12)						
P. ponderosa	hb-1-b	0.71076	4	2.8	0.62	5.8
P. ponderosa	hb-1-c	0.71128	12	3.4		
P. ponderosa	hb-1-e	0.71095	8	2.6	0.48	4.0
P. ponderosa	hb-1-k	0.71051	7	3.1	0.55	5.6
P. ponderosa	hb-2	0.71127	11	4.3		
La Plata Mountains						
Site 220 N37°15.296′ W108°00.139′ 2397 m						
P. ponderosa	lpm-220a	0.71071	19	4.2	0.45	6.3
P. ponderosa	lpm-220b	0.71125	15	3.3	0.55	6.1
P. ponderosa	lpm-220c	0.70985	6	3.6	0.48	5.7
P. ponderosa	lpm-220d	0.71037	5	4.5	0.44	6.7
P. ponderosa	lpm-220e	0.71067	9	3.0	0.42	4.1
Site 222 N37°20.614′ W107°41.586′ 2736 m						
Abies engelmanii	lpm-222a	0.70947	14	5.0		
Populus tremuloides	lpm-222b	0.70954	4	4.3		
Populus tremuloides	lpm-222c	0.70964	39	3.9		
Abies lasiocarpa	lpm-222b	0.70865	19	1.8		
Site 223 N37°17.991′ W107°56.351′ 2228 m						
P. ponderosa	lpm-223a	0.70939	16	2.7	0.56	5.1
P. ponderosa	lpm-223a	0.70939	11	3.5	0.25	2.9
P. ponderosa	lpm-223b	0.70934	18	3.5	0.48	5.6
P. ponderosa	lpm-223c	0.70982	24	4.3		
P. ponderosa	lpm-223c	0.70972	10	1.8		
Site 224 N37°12.573′ W107°18.862′ 2092 m						
P. ponderosa	lpm-224c	0.71102	24	6.63		
P. ponderosa	lpm-224c	0.71093	9	4.4		
P. ponderosa	lpm-224d	0.71131	13	8.4	0.41	11.4
San Juan Mountains						
Site 225 N37°17.864′ W107°20.103′ 2349 m						
Abies engelmanii	sj-225e	0.71057	9	4.5		
Abies concolor	sj-225b	0.71036	7	1.8		
Abies concolor	sj-225a	0.71066	12	29.6		
Cuba Mesa						
Site 226 N36°03.94′ W106°59.837′ 2252 m						
P. ponderosa	cu-226a	0.71390	31	0.9	0.79	2.3
P. ponderosa	cu-226b	0.71431	34	4.6		
P. ponderosa	cu-226c	0.71417	36	3.9		
P. ponderosa	cu-226d	0.71413	10	2.2	0.41	3.0
P. ponderosa	cu-226e	0.71395	40	4.8	0.42	6.7
San Pedro Mountains						
Site 227 N35°59.574′ W106°52.624′ 2436 m						
P. ponderosa	spm-227a	0.71803	10	2.0	0.26	1.7
P. ponderosa	spm-227b	0.71901	11	6.1	0.24	4.9
P. ponderosa	spm-227c	0.71918	4	7.3		
P. ponderosa	spm-227d	0.71557	11	1.5	0.60	3.0
P. ponderosa	spm-227e	0.71613	60	4.0	0.39	5.2
Lybrook						
Site 228 N36°15.625′ W107°39.252′ 2196 m						
P. ponderosa	ly-228a	0.70867	6	7.5	0.62	15.5
Chaco Canyon						
P. ponderosa	jpb-99	0.70943	6	28.7		

$2\sigma^*$ uncertainties correspond to the last two significant figures of the isotope ratio. $^{87}Sr/^{86}Sr^*$ equals $(^{87}Sr/^{86}Sr)_{measured}$ corrected to 0.710235. BD_{wood} = weight of wood (g)/volume of wood (cm^3) by caliper measurements.

[1] In order to correct the Sr (ppm) for water content differences in the wood, the product of Sr concentration and bulk density of the sample was normalized to architectural bulk density average (0.299663).

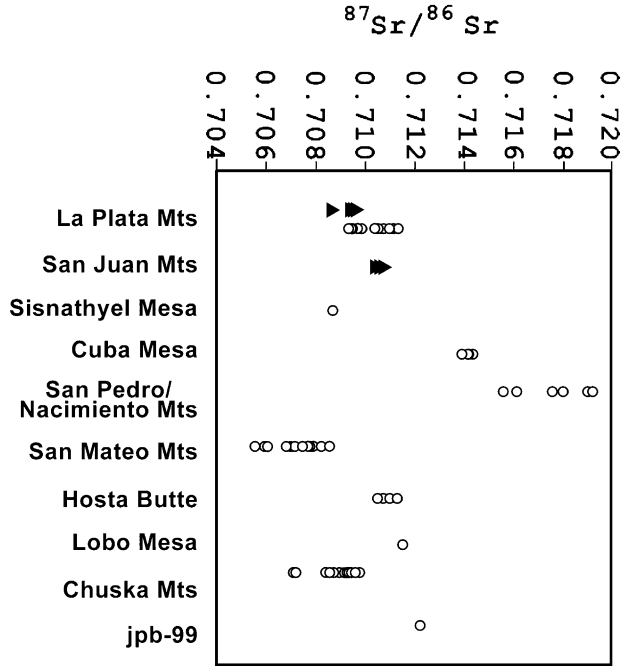

Fig. 4. $^{87}Sr/^{86}Sr$ ratios for living ponderosa pine and spruce/fir species sampled from sites located in Fig. 1. For the spruce/fir, only the San Juan Mountains (Site 225 in Fig. 1) is from this study. All other spruce/fir values are from English et al. [17].

ponderosa match the overlap in $^{87}Sr/^{86}Sr$ (0.7094–0.7097) between the La Platas/San Juans and the Chuska Mountains. About 20% of the architectural ponderosa fall below (0.7084–0.7093) this overlap, but still within the range of living trees in the Chuska Mountains. Nearly half of the architectural ponderosa fall within the $^{87}Sr/^{86}Sr$ range of predicted soil waters for Chaco Canyon (0.70896–0.70961) from Benson et al. [4]. One secondary beam from Pueblo Bonito (cnm-2079: 0.7118) does not correspond to the ranges of values for living trees, and no architectural ponderosa have values <0.7071 that might correspond to the San Mateo Mountains. Judd's "rooted" ponderosa (JPB-99) from the West Plaza of Pueblo Bonito has an isotopic ratio ($^{87}Sr/^{86}Sr = 0.7094$) that cannot be discriminated among Chaco Canyon (ratios reported in Ref. [4] and Reynolds, Betancourt and Akins, unpublished data), the Chuska or La Plata Mountains. Thus, we cannot determine isotopically if Pueblo Bonito was built around this lone living ponderosa or if the dead timber (with roots intact) was placed later into the site.

Some weak patterns are evident in $^{87}Sr/^{86}Sr$ values distributed by great house (Fig. 5) and cutting date (Fig. 6), though interpretation is confounded by our relatively limited sample ($N = 48$). The wide range of isotopic values of ponderosa timber in each of the great houses suggests the use of common stockpiles, and possibly the recycling of constructional timber across sites. When plotted against their cutting dates in the 11th century for the combined great houses and discounting a few outliers, the architectural ponderosa variability is greatest in A.D. 1070–1080 (Fig. 6).

In the architectural samples, mean Sr concentration is 11.6 ± 15.5 ppm (1 standard deviation). The large standard deviation is primarily due to two samples in the architectural wood with extremely high ppm concentrations, cnm-3408 at Pueblo del Arroyo (107 ppm) and cnm-4191 at Chetro Ketl (42 ppm). Without these outliers, the mean concentration becomes 9.8 ± 7 ppm. In the living trees, Sr concentrations, corrected for bulk density, average 7.8 ± 4.8 ppm. Average Sr concentrations in both the architectural and living samples overlap.

5. Discussion

5.1. Testing for diagenesis in the architectural samples

When analyzing the chemistry of architectural specimens, diagenetic contamination (especially secondary salts) is always a concern, particularly in porous materials such as wood and bone. To test for diagenetic additions in the architectural wood, we (1) plotted Sr concentrations against $^{87}Sr/^{86}Sr$ values, and (2) compared the Sr concentrations in the architectural wood to those in the living specimens, with the assumption that pristine archaeological samples should yield comparable concentrations. If Sr additions did occur, higher Sr concentrations will be seen in the architectural samples and those Sr additions will bias $^{87}Sr/^{86}Sr$ ratios towards the ratio of the contaminant, in this case, Chaco Canyon soil water values (0.7094). As stated previously, architectural and living tree Sr concentrations overlap considerably, implying little to no Sr additions. And, as seen in Fig. 7, very little or no correlation exists between $^{87}Sr/^{86}Sr$ ratios and concentrations. This rules out the possibility that architectural $^{87}Sr/^{86}Sr$ ratios have been systematically altered towards the ratios of local soil water. Although diagenetic effects have been considered for bones and teeth [22], they had not been considered previously for archaeobotanical materials.

5.2. Comparison of living and architectural ponderosa and spruce/fir

By way of synthesis, we compare our $^{87}Sr/^{86}Sr$ values for both living and architectural ponderosa with those reported for spruce and fir in English et al. [17] (Fig. 8). We lump spruce and fir in a single category because they tend to occur together in the region, and the architectural timber probably comes from these mixed stands. In general, the isotopic ratios for ponderosa match those for spruce and fir growing at the same localities. One

Table 2
Summary of architectural ponderosa samples, including name of great house, room designation, function, age, $^{87}Sr/^{86}Sr$ ratios, and Sr concentration

Sample ID	Cutting date (A.D.)	Genus	Room	Function	$^{87}Sr/^{86}Sr$*	2σ*	ppm
Pueblo Bonito							
cnm-2079	1080	pp	171	Secondary	0.71176	11	4.6
cnm-2636	1030	pp	299	Primary	0.70984	33	9.8
cnm-2642	1029	pp	300	Primary	0.70968	33	25.5
pb-290	1080	pp	227	Secondary	0.70950	9	3.9
pb-294	1082	pp	227	Secondary	0.70958	10	5.7
pb-304	1081	pp	317	Vent lintel	0.70927	10	18.2
pb-34	919	pp	320	Secondary	0.70953	3	11.7
pb-341	1081	pp	320	Door lintel	0.70930	10	20.2
pb-356	1081	pp	326	Door lintel	0.70958	23	4.7
pb-460	1049	pop	100a	Door lintel	0.71054	11	9.6
pb-512	1046	pp	209	Door lintel	0.71008	19	8.2
pb-532	1080	pp	242	Door lintel	0.70930	7	9.3
pb-540	1080**	pp	244	Door lintel	0.71034	11	1.8
pb-577	1029	pp	299	Primary	0.70984	10	7.6
pb-581	1030	pp	299	Primary	0.70989	58	8.9
ckk-40 nps	1081	pp	7 (KK)	Door lintel	0.71002	11	3.0
ckk-41 nps	1081	pp	7 (KK)	Door lintel	0.71000	8	4.6
ckk-72 nps	1081	pp	25 (KK)	Door lintel	0.71574	14	2.5
cnm-3338 nps	1029	pp	Kiva G (PB)	Tie beam	0.70930	7	10.7
cnm-3453 nps	1081	pp	49 (KK)	Vent lintel	0.70864	11	26.0
cnm-3455 nps	1081	pp	49 (KK)	Vent lintel	0.70949	28	8.0
Chetro Ketl							
ck-1165	1042	pp	46/48	Lintel	0.70940	11	3.8
ck-1224	1051	pp	39A	Secondary	0.70960	33	4.3
ck-1225	1052	pp	39A	Secondary	0.71068	8	4.1
ck-1226	1051	pp	39A	Secondary	0.70949	5	25.5
ck-1232	1034	pp	39A	Secondary	0.70940	13	24.0
ck-1233	1052	pp	39A	Secondary	0.70953	24	13.0
ck-1239	1052	pp	39A	Secondary	0.71102	7	6.0
ck-1275	1033	pp	92	Primary	0.70928	6	11.9
ck-1300	1033	pp	106	Beam 11	0.71697	22	3.5
ck-1303	1033	pp	106	Beam 14	0.70919	12	13.8
ck-1307	1034	pp	106	Beam 18	0.71028	35	5.2
cnm-4133	1048	pp	114	Primary	0.71018	25	0.4
cnm-4191	1051	pp	119	Primary	0.71001	42	42.1
cnm-4192	1048	pp	119	Primary	0.70972	12	7.9
cnm-2504	1039	pp	40 (PdA)	Primary	0.70957	36	2.6
ck-1144 nps	1043	pp	43 (CK)	Primary	0.70951	24	7.5
cnm-1492 nps	1043	pp	37 (PdA)	Primary	0.70916	10	14.3
cnm-1617 nps	1038	pp	87 (PdA)	Vent lintel	0.70960	47	5.3
cnm-1678 nps	1037	pp	144 (PdA)	Primary	0.70978	28	4.2
Pueblo del Arroyo							
cnm-1186	1077	pp	43	Lintel	0.71096	26	1.8
cnm-1187	1076	pp	43	Lintel	0.71011	22	4.8
cnm-1188	1077	pp	43	Lintel	0.70997	8	8.8
cnm-1363	1101	pp	8	Door lintel	0.70917	25	4.7
cnm-1377	1100	pp	9A III	Primary	0.71016	19	16.1
cnm-1390	1100	pp	9A III	Secondary	0.70839	16	0.4
cnm-1392	1099	pp	9A III	Secondary	0.70946	14	2.7
cnm-1393	1100	pp	9A	Secondary	0.70981	27	1.2
cnm-1405	1099	pp	9A III	Secondary	0.70957	10	4.3
cnm-1649	1076	pp	102	Primary	0.70949	6	14.1
cnm-2525	1099	pp	43	Primary	0.71043	11	10.7
cnm-3408	1071	pp	95	Intramural	0.70919	19	107.0

2σ* uncertainties correspond to the last two significant figures of the isotope ratio. $^{87}Sr/^{86}Sr$* equals $(^{87}Sr/^{86}Sr)_{measured}$ corrected to 0.710235. **Tentative cuting date. ''nps'' listed after a sample name indicates reused wood in National Park Service stabilization efforts. Such beams are categorized according to the beam's original great house. The present location of the beam is indicated in parentheses under the ''room'' column (PB = Pueblo Bonito, CK = Chetro Ketl, KK = Kin Kletso, and PdA = Pueblo del Arroyo).

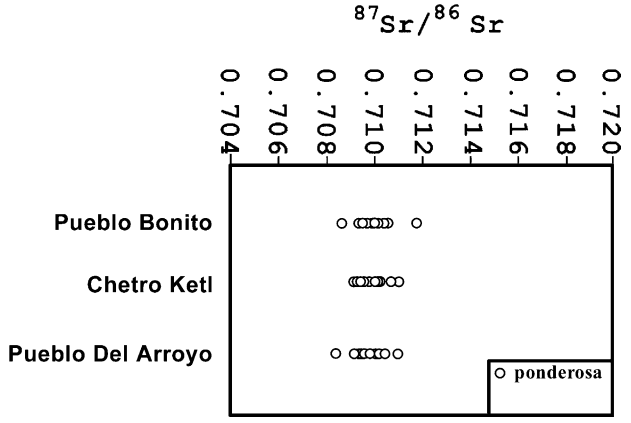

Fig. 5. $^{87}Sr/^{86}Sr$ ratios for architectural ponderosa pine from three great houses [Pueblo Bonito, Chetro Ketl, and Pueblo Del Arroyo].

exception is the lower $^{87}Sr/^{86}Sr$ value of the Abies sample from site 222 in the La Plata Mountains which may be an anomalous sample or reflects a species effect. Another exception is the higher $^{87}Sr/^{86}Sr$ ratios for ponderosa in the San Pedro/Nacimiento Mountains, which may have to do more with substrate than species effects.

The greatest aerial exposure of bedrock in the San Pedro/Nacimiento Mountains is a compositionally-diverse array of Precambrian crystalline rock, but in the southern sector (the Nacimiento Mountains) there are limited outcrops of Paleozoic limestones and sandstones. English et al. [17] found little difference in the spruce and fir growing on three substrates (granite, limestone, and sandstone) in the San Pedro/Nacimiento Mountains, suggesting atmospheric dust as the primary source of plant-available Sr. The higher $^{87}Sr/^{86}Sr$ ratios for ponderosa, however, came from trees growing on soils developed from the Permian Abo Sandstone, which at our sampling locality was derived from erosion of local, uplifted Precambrian blocks of granite [37]. At our sampling site, the Abo rests directly on Precambrian granite, and the closest surface exposures of this

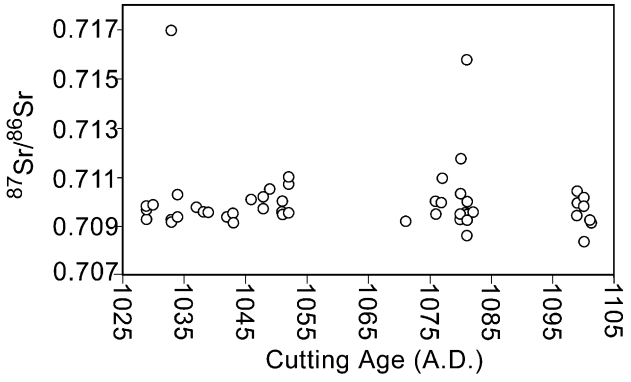

Fig. 6. Cutting dates plotted against the $^{87}Sr/^{86}Sr$ ratios of architectural ponderosa pine.

bedrock are ~2 km northwest and southwest of our sampling sites. Therefore, one explanation for trees having generally higher $^{87}Sr/^{86}Sr$ ratios on Abo Sandstone (0.7156–0.7190) than on Precambrian granite (0.7130–0.7170) [17] may be a greater bioavailability of Sr weathering products in granite-derived alluvium than in granite bedrock. The finer grain size of the Abo Sandstone, however, provides greater surface area for chemical weathering. Compared to outcrops of Precambrian granite, Abo Sandstone may contribute greater amounts of Sr to soil water from bedrock weathering than from atmospheric dust, which generally contains a mixture of local and regional sources.

Of the 52 architectural samples that were analyzed in this study, half of the beams (26 beams) have $^{87}Sr/^{86}Sr$ ratios that fall in the zone of overlap among Chaco Canyon soil waters and the La Plata and Chuska Mountains (0.70896–0.7097). A timber source from Chaco Canyon, itself, is unlikely; the extensive packrat midden record from local cliffs shows a paucity of ponderosa pine during Anasazi occupation [6]. With the exception of two secondary samples that fall in the range of the southern Chuska Mountains, the other half of architectural beams conform to the higher ratios seen in the La Plata and San Juan Mountains and surrounding mesas. This distribution is the same across Pueblo Bonito, Chetro Ketl, and Pueblo del Arroyo great houses. While the Sr isotopic ratios are not enough to pinpoint the source of Chacoan architectural timber, the ponderosa pine data are discriminating its sources away from the south and more to northwestern and northern sources. Beams of various ages and functions all show similar distribution.

The overlap among $^{87}Sr/^{86}Sr$ wood ratios of potential source stands between the Chuskas and La Platas limits determination of exact sources for the architectural timber. Ambiguities in the data could be overcome by supplementing $^{87}Sr/^{86}Sr$ ratios with elemental concentration (e.g., barium) and/or other radiogenic isotopes from elements with living wood concentrations that exceed 100 ppb (e.g., sulphur and lead, but not neodymium, which in wood occurs in very low concentration).

For the sake of comparison, $^{87}Sr/^{86}Sr$ ratios for all three conifers are available from three of the ruins (Pueblo Bonito, Chetro Ketl and Pueblo del Arroyo). The ratios for ponderosa and spruce/fir (mostly contemporaneous in cutting age) are very similar for Pueblo del Arroyo, but many of the ponderosa beams at Pueblo Bonito and Chetro Ketl have higher $^{87}Sr/^{86}Sr$ ratios than the range for spruce/fir (Fig. 9). Much of the architectural timber, whether spruce–fir or ponderosa, could have come from the Chuska Mountains. The lowest $^{87}Sr/^{86}Sr$ ratios for spruce/fir from Pueblo Bonito and Chetro Ketl, however, most closely match living trees from the San Mateo Mountains. The higher

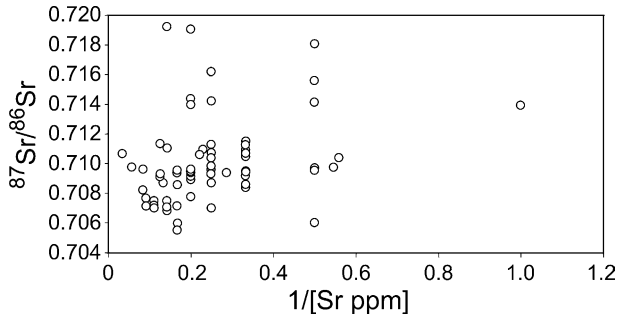

Fig. 7. Plot of $^{87}Sr/^{86}Sr$ ratios against Sr concentration (ppm) for architectural ponderosa pine to argue against simple mixing between two end members, or diagenetic effects.

$^{87}Sr/^{86}Sr$ ratios in ponderosa at these two great houses, on the other hand, best match living trees in the La Plata/San Juan Mountains. Some of the higher $^{87}Sr/^{86}Sr$ ratios for ponderosa samples at Pueblo Bonito and Chetro Ketl also match Hosta Butte and Lobo Mesa.

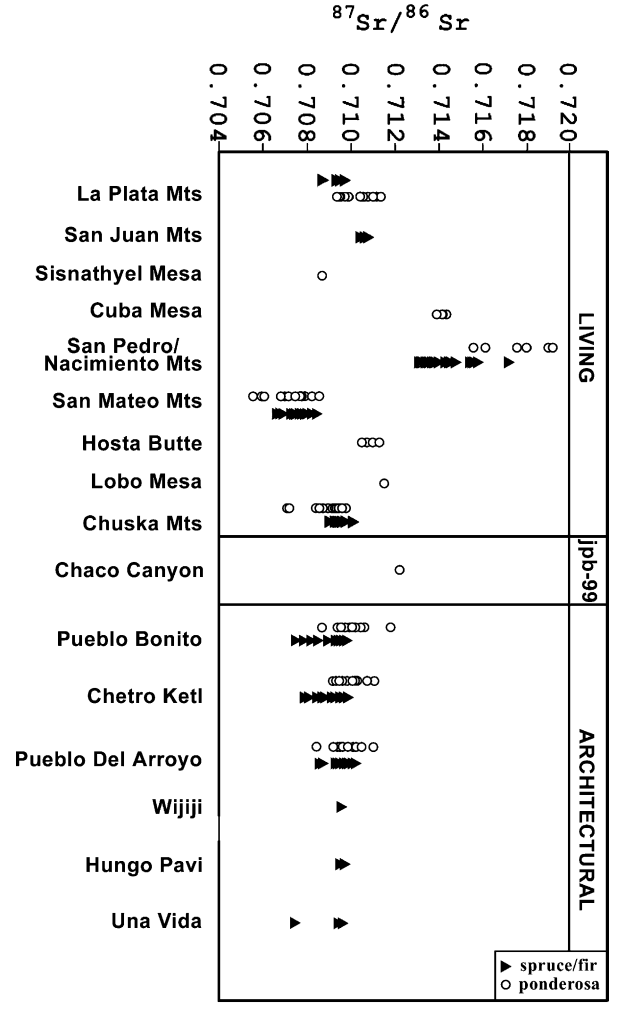

Fig. 8. Summary plot of $^{87}Sr/^{86}Sr$ ratios for both living and architectural ponderosa pine (circles) and spruce/fir (triangles) from English et al. [17] study.

We wonder, however, why stands of ponderosa on Hosta Butte would have been harvested, whereas those on the northern flanks of the San Mateo Mountains, which provided some of the spruce/fir, were not exploited. Alternatively, we suggest that the wood with higher $^{87}Sr/^{86}Sr$ ratios from Pueblo Bonito and Chetro Ketl actually comes from the north in the southern foothills and mesas of the La Plata and San Juan Mountains. We recognize that this would have involved the questionable rafting of timber across the San Juan River, and leave open the possibility that the wood came from other more accessible areas that we failed to sample. Ponderosa beams with higher $^{87}Sr/^{86}Sr$ ratios from Pueblo del Arroyo could have come from granite or granite-derived fluvial sandstones to the north (in the La Plata or San Juan Mountains) or the San Pedro/Nacimiento Mountains to the east. Finally, the only clear trend in time, seen only at Chetro Ketl, is a shift in mean Sr ratios at A.D. 1050. Timbers are dominated by ponderosa with higher $^{87}Sr/^{86}Sr$ ratios prior to A.D. 1050 and by spruce/fir with lower $^{87}Sr/^{86}Sr$ ratios after that time. We do not think this is a sampling artifact, nor is the difference in ratios likely due to change in species use because large-scale ponderosa and spruce/fir procurement spans this period. It could be related to a change in procurement locus or, more likely, expansion of procurement loci during a major building boom at Chetro Ketl that began around A.D. 1050.

The Chuska Mountains seem to have been the preferred source area for spruce, fir and ponderosa, but our sampling was concentrated in the middle of the mountain range closest to Chaco Canyon. This leaves open the possibility that some of the wood we are attributing to the La Plata and San Juan Mountains or Hosta Butte actually came from the north (the Lukachukai and Carrizo Mountains). We acknowledge that our sampling of living trees was spotty and we may have missed many potential source stands.

6. Conclusions

Strontium isotopic analyses indicate that the architectural ponderosa used in three of the Chacoan great houses likely came mostly from the Chuska Mountains to the west and the La Plata and San Juan Mountains to the north and possibly Hosta Butte to the south. A previous study showed that spruce and fir in six of the great houses came mostly from the Chuska Mountains, with some contributions from the San Mateo Mountains to the south. Comparison between ponderosa and spruce/fir architectural samples indicates that great house construction may have been provisioned from three general directions, but not from the east.

In the geologically-diverse San Juan Basin, variation in $^{87}Sr/^{86}Sr$ of trees is highly dependent on the properties

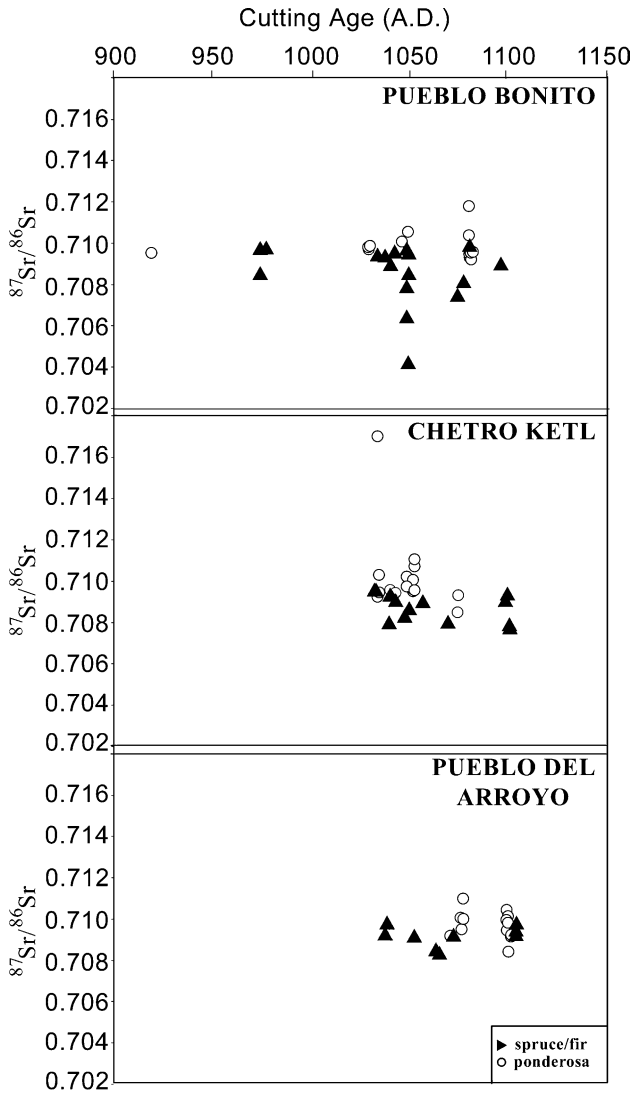

Fig. 9. Summary plot of cutting dates for architectural ponderosa (circles) and spruce/fir (triangles) from English et al. [17] study plotted against their respective $^{87}Sr/^{86}Sr$ ratios.

of the bedrock (e.g., chemical weathering rates) and relative contributions from atmospheric inputs. Atmospheric inputs tend to homogenize Sr ratios across different bedrock types in close proximity, with rapidly weathering bedrock types producing greater heterogeneity. Our broadbrush approach to characterizing plant $^{87}Sr/^{86}Sr$ across the San Juan Basin ignores local nuances in surficial geology, and there are surely many blind spots and uncertainties in our provenance studies thus far.

To date there have been surprisingly few synoptic and intensive $^{87}Sr/^{86}Sr$ sampling of bedrock, soil and soil water, and plants [21] to produce comprehensive baselines for provenance studies in archeology. Thus, we encourage continued expansion of the growing database for the San Juan Basin, and its application to better understanding of the provision and distribution of both plant and animal materials throughout the Chacoan system. It is becoming increasingly evident that the multiple sources of arcaeobotanical materials recovered from Chaco Canyon would have been underestimated by analysis of just one species, a single class of artifact, or only a few isotopic values.

Acknowledgments

We thank Taft Blackhorse for collection of samples from Hosta Butte, Nathan English and Clark Isachsen for advice on lab protocols, and Dick Warren for help with retrieving archived samples. We also thank Bruce Allen for discussions on the nuances of New Mexico geology, and Tom Windes and Camille Holmgren, and four anonymous reviewers for comments on the manuscript. This work was funded by the Chaco Sites Protection Program of the Navajo Nation, the U.S. Geological Survey, and an NSF-IGERT Fellowship in Archaeometry at the University of Arizona (to ACR). Sampling permits were granted graciously by the Navajo Nation, the USDA Forest Service, and the National Park Service.

References

[1] G. Åberg, G. Jacks, T. Wickman, P. Hamilton, Strontium isotopes in trees as an indicator of calcium availability, Catena 17 (1990) 1–11.
[2] L. Augusto, M.-P. Turpault, J. Ranger, Impact of forest tree species on feldspar weathering rates, Geoderma 96 (2000) 215–237.
[3] G. Barci-Funel, J. Dalmasso, V.L. Barci, G. Ardisson, Study of the transfer of radionuclides in trees at a forest site, Sci. Total Environ. 173/174 (1995) 369–373.
[4] L. Benson, L. Cordell, K. Vincent, H. Taylor, J. Stein, G.L. Farmer, K. Futa, Ancient maize from Chacoan great houses: Where was it grown? Proc. Natl Acad. Sci. 100 (2003) 13111–13115.
[5] J.L. Betancourt, J.S. Dean, H.M. Hull, Prehistoric long distance transport of construction beams, Chaco Canyon, New Mexico, Am. Antiquity 51 (1986) 370–375.
[6] J.L. Betancourt, T.R. Van Devender, R.S. Martin, Fossil packrat middens from Chaco Canyon, New Mexico: cultural and ecological significance, in: S.G. Wells, D.W. Love, T.W. Gardner (Eds.), Chaco Canyon Country, A Field Guide to the Geomorphology, Quaternary Geology, Paleoecology, and Environmental Geology of Northwestern New Mexico, American Geomorphological Field Group, Albuquerque, 1983, pp. 207–217.
[7] J.D. Blum, A. Klaue, C.A. Nezat, C.T. Driscoll, C.E. Johnson, T.G. Siccama, C. Eagar, T.J. Fahey, G. Likens, Mycorrhizal weathering of apatite as an important calcium source in base-poor forest ecosystems, Nature 417 (2002) 729–731.
[8] J.D. Blum, E.H. Taliaferro, M.T. Weisse, R.T. Holmes, Changes in Sr/Ca, Ba/Ca, and $^{87}Sr/^{86}Sr$ ratios between trophic levels in two forest ecosystems in the northeastern U.S.A. Biogeochemistry 49 (2000) 87–101.
[9] E.A. Bondietti, C.F. Baes III, S.B. McLaughlin, Radial trends in cation ratios in tree rings as indicators of the impact of

atmospheric deposition on forests, Can. J. For. Res. 19 (1989) 586–594.
[10] R. Capo, B. Stewart, O. Chadwick, Strontium isotopes as tracers of ecosystem processes: Theory and methods, Geoderma 82 (1998) 197–225.
[11] O.A. Chadwick, L.A. Derry, P.M. Vitousek, B.J. Huebert, L.O. Hedin, Changing sources on nutrients during four million years of ecosystem development, Nature 397 (1999) 491–497.
[12] S.D. Craigg, Geologic framework of the San Juan structural basin of New Mexico, Colorado, Arizona, and Utah with emphasis on Triassic through Tertiary rocks: regional aquifer-System analysis, U.S. Geological Survey Prof. Paper 1420 (2001).
[13] L.S. Crumpler, Volcanism in the Mount Taylor region, in: J.A. Grambing, S.G. Well (Eds.), Albuquerque Country II 33rd Annual Field Conference, New Mexico Geological Society, Albuquerque, 1982, pp. 291–298.
[14] J.S. Dean, R.L. Warren, Dendrochronology, in: S.H. Lekson (Ed.), Architecture and Dendrochronology of Chetro Ketl, Chaco Canyon, New Mexico, Reports of the Chaco Center, No. 6, Division of Cultural Research, National Park Service, Albuquerque, 1983, pp. 105–240.
[15] D.R. DeWalle, W.E. Sharpe, B.R. Swistock, Dendrochemistry and the soil chemical environment, in: T.E. Lewis (Ed.), Tree Rings and Indicators of Ecosystem Health, 1995, pp. 81–93 (Chapter 4).
[16] S.R. Durand, P.H. Shelley, R.C. Antweiler, H.E. Taylor, Trees, chemistry, and prehistory in the American Southwest, J. Archaeol. Sci. 26 (1999) 185–203.
[17] N. English, J. Betancourt, J. Dean, J. Quade, Strontium isotopes reveal distant sources of architectural timber in Chaco Canyon, New Mexico, Proc. Natl Acad. Sci. 98 (2001) 11891–11896.
[18] W.C. Graustein, R.L. Armstrong, The use of strontium-87/strontium-86 ratios to measure atmospheric transport in forested watersheds, Nature 219 (1983) 289–292.
[19] W.C. Graustein, $^{87}Sr/^{86}Sr$ ratios measure the sources and flow of strontium in terrestrial ecosystems, in: P.W. Rundel, J.R. Ehleringer, K.A. Nagy (Eds.), Stable Isotopes in Ecological Research, Springer-Verlag, New York, 1989, pp. 491–512.
[20] S.H. Hatch, A wood sourcing study at the Chimney Rock Archaeological Area Southwest Colorado, MA thesis in Anthropology at Northern Arizona University, Flagstaff AZ, 1994, 237 pp.
[21] D.A. Hodell, R.L. Quinn, M. Brenner, G. Kamenov, Spatial variation of strontium isotopes ($^{87}Sr/^{86}Sr$) in the Maya region: a tool for tracking ancient human migration, J. Archaeol. Sci. 31 (2004) 585–601.
[22] K.A. Hoppe, P.L. Koch, T.T. Furutani, Assessing the preservation of biogenic strontium in fossil bones and tooth enamel, Int. J. Osteoarchaeol. 13 (2003) 20–28.
[23] N.M. Judd, The architecture of Pueblo Bonito, Smithsonian Miscellaneous Collections 147 (1), Washington, D.C.: Smithsonian Institution (1964).
[24] J. Kantner, An Evaluation of Chaco Anasazi Roadways, Paper Presented in the Current Technology Applied to Archaeology Poster Session, 61st Society for American Archaeology Annual Meeting, New Orleans, Louisiana, April 11, 1996.
[25] M.J. Kennedy, L.O. Hedin, L.A. Derry, Decoupling of unpolluted temperate forests from rock nutrient sources revealed by natural $^{87}Sr/^{86}Sr$ and ^{84}Sr tracer addition, Proc. Natl Acad. Sci. 99 (2002) 9639–9644.
[26] B. Markert, The biological system of the elements (BSE) for terrestrial plants (glycophytes), Sci. Total Environ. 155 (1994) 221–228.
[27] N.R. Miller, D.R. Denison, R.W. Scott, D.F. Reaser, Strontium isotope stratigraphy of the Comanchean series in North Texas, Geological Society of America, 2001 Annual Meeting, 33 (2001) 444. Geological Society of America (GSA), Boulder, CO, United States.
[28] Z. Naiman, J. Quade, P.J. Patchett, Isotopic evidence for eolian recycling of pedogenic carbonate and variations in carbonate dust sources throughout the southwest United States, Geochim. Cosmochim. Acta 64 (2000) 3099–3109.
[29] T.D. Price, C.M. Johnson, J.A. Ezzo, J. Ericson, J.H. Burton, Residential mobility in the prehistoric southwest United States: A preliminary study using strontium isotope analysis, J. Archaeol. Sci. 21 (1994) 315–330.
[30] R. Reynolds, J. Belnap, M. Reheis, P. Lamothe, F. Luiszer, Aeolian dust in Colorado Plateau soils: nutrient inputs and recent change in source, Proc. Natl Acad. Sci. 98 (2001) 7123–7127.
[31] K.T. Smith, W.C. Shortle, Tree biology and dendrochemistry, in: J.S. Dean, D.M. Meko, T.W. Swetnam (Eds.), Tree Rings, Environment, and Humanity, Radiocarbon (1996) 629–635.
[32] B.W. Stewart, R.C. Capo, O.A. Chadwick, Effects of rainfall on weathering rate, base cation provenance, and Sr isotope composition of Hawaiian soils, Geochim. Cosmochim. Acta 65 (2001) 1087–1099.
[33] S. Van der Hoven, J. Quade, Tracing spatial and temporal variations in the sources of calcium in pedogenic carbonates in a semi-arid environment, Geoderma 108 (2002) 259–276.
[34] R.G. Vivian, Chacoan roads: morphology, Kiva 63 (1997) 1–34.
[35] T.C. Windes, P.J. McKenna, Going against the grain: wood production in Chacoan society, Am. Antiquity 66 (2001) 119–140.
[36] T.C. Windes, D. Ford, The Chaco wood project: the chronometric reappraisal of Pueblo Bonito, Am. Antiquity 61 (1996) 295–310.
[37] L.A. Woodward, Geology and mineral resources of Sierra Nacimiento and vicinity, New Mexico: NM Bureau of Mines and Mineral Resources, Memoir 42, 1987, 84 pp. plus map.